communications medicine

A Nature Portfolio journal

Article

https://doi.org/10.1038/s43856-025-01212-y

The role of the salience network in adolescent impulsivity using memory tasks and neuroimaging

Jae-Chang Kim[1], Kyeong Seob Song[2], Jinyoung Kim[3], Minkyung Hu[3], Joong Il Kim[4,5], In Young Choi[2], Tae Min Kim[2,6], Dai-Jin Kim[3] & Ji-Won Chun[2,6]

Abstract

Background This study investigated potential behavioral and neural biomarkers of adolescent impulsivity by analyzing adolescent responses in a memory test and examining task-independent brain connectivity.

Methods This research utilized immediate and delayed memory tasks, together with a similar distractor memory task (SMT), to examine adolescent impulsivity and its correlation with neural cognitive control strategies. Ninety-five healthy, right-handed teenagers (27 females, average age 14.9 years) participated in the functional magnetic resonance imaging (fMRI) sessions.

Results Elevated impulsivity correlates with an increased number of errors during target trials and a higher incidence of false alarms during catch trials. Neural activity and connectivity involving the insula and dorsal anterior cingulate cortex (dACC) are significantly associated with behavioral responses and individual impulsivity. Notably, both task-modulated and resting-state (intrinsic) coupling between the insula and locus coeruleus (LC), as well as between the dACC and LC, demonstrate significant positive correlation with impulsivity. These findings indicate that insula-LC and dACC-LC connectivity strength serve as reliable indicators of impulsivity.

Conclusions The results indicate that the connection between the salience network and the noradrenergic locus coeruleus may function as a consistent neural indicator of impulsivity. Our findings indicate that this method can discern reliable brain biomarkers for impulsivity and can guide interventions aimed at enhancing self-control during adolescence.

Plain language summary

Teenagers often display impulsivity during adolescence, which is linked to risky decisions and mental health problems. Our study examined how brain systems involved in impulse control relate to impulsive behavior in teenagers. Using functional MRI, we measured brain activity while 95 healthy adolescents completed delayed memory tasks. We found that more impulsive adolescents made more errors on these tasks. In the brain, this was associated with the salience network (specifically the insula and dorsal anterior cingulate cortex). Furthermore, ongoing connections between the salience network and the noradrenergic locus coeruleus show a significant link to impulsivity, both during the task and at rest. These findings suggest potential neurological markers that could help develop future strategies to support self-control in teenagers.

Impulsivity in adolescents is closely linked to dangerous behaviors such as substance abuse, unprotected sexual activity, and delinquency, making it a critical area of study[1–4]. These impulsive behaviors are often attributed to a developmental imbalance between an underdeveloped cognitive control system and a highly responsive affective processing system[5,6]. Impulsivity, defined as the tendency to act without considering future consequences, can undermine the development of critical self-regulating abilities, including executive function and impulse control[7].

Extensive research demonstrates that the neural mechanisms underlying inhibitory control undergo significant maturation during adolescence. For example, increased prefrontal–anterior cingulate connectivity has been observed[8], delayed frontal recruitment in adolescents has been reported[9], and reward-related striatal modulation of inhibitory control has been documented in teens[10]. Furthermore, prolonged development of error-processing systems[11] and altered frontal activation linked to impulsivity in vulnerable youth[12] emphasize the dynamic nature of this maturation.

[1]Zurich Center for Neuroeconomics, Department of Economics, University of Zurich, Zurich, Switzerland. [2]Department of Medical Informatics, The Catholic University of Korea College of Medicine, Seoul, Republic of Korea. [3]Department of Psychiatry, Seoul St. Mary's Hospital, The Catholic University of Korea College of Medicine, Seoul, Republic of Korea. [4]Digital Health Research Division, Korea Institute of Oriental Medicine, Daejeon, South Korea. [5]Korean Convergence Medical Science, University of Science and Technology, Daejeon, South Korea. [6]CMC Institute for Basic Medical Science, The Catholic Medical Center of The Catholic University of Korea, Seoul, Republic of Korea. e-mail: jwchun@catholic.ac.kr

At the same time, the salience network (SN), which mainly includes the anterior insula and anterior cingulate cortex, gets significantly increased connectivity both within and across network during the teenage years[13]. Longitudinal studies indicate that the within-network connectivity of the SN generally increases with age, enhancing the brain's capacity to detect and integrate salient stimuli[14]. Enhanced SN connectivity is associated with improved cognitive control and reduced impulsivity[15], whereas disruptions or delayed maturation of the SN have been linked to heightened impulsivity and increased vulnerability to risky behaviors[16]. Clarifying the impact of SN maturation on impulsivity is crucial for understanding adolescent behavior.

Traditional inhibitory control tasks, such as the Stop-signal and Go/No-go paradigms[17], typically compare successful and failed inhibition. In contrast, our initial paradigm, which integrated immediate and delayed memory tasks, focused on memory and attention rather than isolating inhibitory control. Notably, our neuroimaging data reveal robust engagement of the SN (i.e., the insula and dorsal anterior cingulate cortex[18,19]) with minimal activation in regions such as the inferior frontal gyrus[20], suggesting that the task predominantly captures attentional control[21,22].

While the connection between the insula and dACC has been thoroughly examined in many cognitive tasks[23–25], their specific roles in response inhibition during memory tasks remain unclear. In addition, the locus coeruleus (LC)–a nucleus that releases norepinephrine[26]–plays a critical role in regulating the SN and affect both the insula and dACC[27–30]. Animal studies have shown that the increasing LC activity via optogenetic activation accelerated task switching[31]. Furthermore, increased pupil diameter, which is a proxy for LC activity, has been found to co-vary with cognitive performance, and fluctuations in LC-linked arousal correspond to variations in attentional control and decision making[21,22]. Together, these findings suggest that LC-mediated modulation of the SN may play a critical role in regulating impulsivity in humans. However, the influence of individual differences in impulsivity on SN-LC connectivity has not been extensively studied in humans.

To fill these gaps in the literature, we developed a unique task paradigm that expands upon conventional immediate- and delayed-memory tasks[32] (IMT and DMT) by incorporating a similar distractor memory task (SMT). The SMT incorporates visual distractors that resemble the cue, which increases cognitive demands and requires accurate discrimination between the cue and the target. This design facilitates thorough evaluations of behavior and includes measurements of both response time and accuracy under various scenarios (IMT, DMT, and SMT). Furthermore, it enables the assessment of inhibitory control in catch trials, where participants are required to refrain from responding despite receiving cue-like prompts.

Our main objective is to examine the relationship between brain activity in the salience network and task performance. We focus on the connections among the insula, dACC, and LC during these tasks. Our goal is to identify consistent brain indicators of impulsivity, as judged by the Barratt Impulsiveness Scale-11 (BIS-11)[33], a measure widely employed in adolescent research[34–37] by studying the connections among behavioral outcomes, neural activity, and connectivity patterns during specific tasks and generally. This methodology not only improves our comprehension of the neurological foundations of impulsivity but also has the potential to facilitate specific interventions to reduce impulsive actions.

Methods

Participants

This study engaged adolescent males and females aged 12 to 18 years through an institutional announcement. Ninety-five healthy, right-handed volunteers (27 females, 12–18 years of age) participated in the functional magnetic resonance imaging (fMRI) sessions of this study. Each participant was provided with $40 for transportation expenses. There was no performance-based compensation in this study. The clinician conducted the Mini-International Neuropsychiatric Interview with all participants to screen out those with a current psychiatric diagnosis. The exclusion criteria included past or current major medical disorders (e.g., diabetes mellitus), neurological disorders (e.g., seizure disorders, head injuries), or psychiatric disorders (e.g., major depressive disorder, anxiety disorders). Imaging data from five subjects was excluded due to detected severe head movements of ±1.5 mm or greater during the realignment phase of preprocessing. Accordingly, we present data from 90 participants (24 females, 14.94 ± 1.7 years). The study was approved by the Research Ethics Committee of the Institutional Review Board at Seoul St. Mary's Hospital, Seoul, South Korea. Written informed consent was obtained from all participants and their parent or legal guardian prior to the experiment.

Psychological measurements

The impulsiveness of the participants was evaluated using the Korean version of the Barratt Impulsiveness Scale-11-Revised (K-BIS-11-R)[38] which is an adaptation of the original Barratt Impulsiveness Scale[33]. The BIS-11 is a 30-item scale that consists of three factors: attentional, motor, and nonplanning impulsivity. The items from the subscales include "I often have extraneous thoughts when thinking" (Attentional), "I act on the spur of the moment" (Motor), and "I am more interested in the present than the future" (Non-planning). Each item is rated on a 4-point Likert-type scale (1=never to 4=always), with higher total scores indicating greater levels of impulsivity. The internal consistency of the K-BIS-11-R was reported as a Cronbach's α of 0.78 with a test-retest reliability of 0.77[38]. The participants' BIS-11 scores (mean ± SEM) were as follows: Total BIS-11 score: 63.04 ± 1.09 (20 participants scored 72 or above, which typically indicates high impulsivity[39]) BIS11_A (Attention): 16.91 ± 0.34; BIS11_M (Motor): 20.94 ± 0.43; and BIS11_NP (Non-Planning): 25.19 ± 0.49. We conducted a correlation analysis between the K-BIS-11-R questionnaire and behavioral reactions as well as functional connectivity. Statistical significance was set at a p-value of 0.05.

Experimental design

The main task included three major task components and was presented using a mixed block design. Each block consisted of the immediate memory task (IMT) and delayed memory task (DMT) based on the impulsivity test, and an additionally designed similar distractor memory task (SMT). Before starting each block, the participants were informed of the type of task they would be performing, either the immediate task or the delayed task.

As shown in Fig. 1 (Task & Neural Activity), the participants were sequentially exposed to a cue stimulus (500 ms) followed by a target stimulus (500 ms), with an interstimulus interval (ISI) of 500 ms during the IMT trials. The participants were instructed to press the button box when the number currently shown on the screen matched the number that was shown immediately before it. In the DMT and SMT trials, a 5-digit number cue was presented, followed by fillers inserted between the cue and target stimuli. In the DMT trials, the fillers presented a fixed number, such as 12345, whereas in the SMT trials, the fillers were similar to the cue trials. Specifically, in the SMT trials, the first digit of the filler was the same as the cue and remained fixed, but one of the remaining four digits was replaced by another digit and then shuffled. Two types of stimuli could be presented during the target phase: a target stimulus (identical to the cue and requiring a response) and a catch stimulus (similar to the cue but requiring no response). After the target stimulus in all task types, a 5-digit filler such as '11111' was presented for 500 ms before the start cue of the next trial. All participants underwent two practice sets that included six blocks to confirm their understanding of this task before the fMRI session.

Prior to the task-based fMRI study, a resting-state fMRI (rsfMRI) session was conducted to investigate the correlation between task-independent connectivity and impulsivity. During the rsfMRI session, the participants fixated their gaze on a crosshair positioned at the center of the screen.

Neuroimaging acquisition and preprocessing

The participants were scanned using a Siemens MAGNETOM Verio 3-Tesla MRI scanner equipped with a 20-channel head coil. During each session, we acquired a series of T2*-weighted echo-planar images (EPI) with voxel dimensions of $2 \times 2 \times 4\ mm^3$ covering a field of view (FOV) of $192 \times 192 \times 72\ mm^3$. The repetition time (TR) was set to 2000 ms, and the echo time (TE) was 30 ms with a flip angle of 90° and a matrix size of 96 × 96. The fMRI sessions involved the acquisition of 316 scans during two sessions

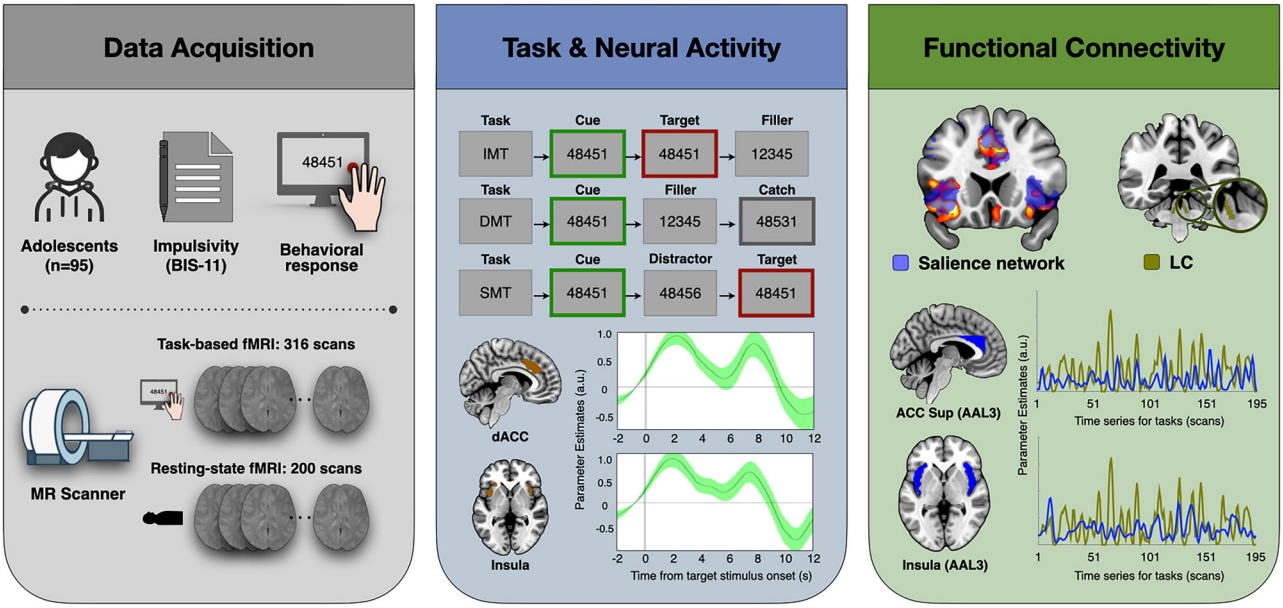

Fig. 1 | Experiment and Analysis Flowchart. Data Acquisition: Ninety-five healthy, right-handed volunteers (27 females) participated in this study's functional magnetic resonance imaging (fMRI) sessions. Impulsiveness was assessed using the Barratt Impulsiveness Scale-11 (BIS-11). Participants completed a resting-state fMRI (rsfMRI) session before engaging in the task-based fMRI study to examine the relationship between task-independent connectivity and impulsivity. Task & Neural Activity: (Top) Example trial structures for the immediate memory task (IMT), delayed memory task (DMT), and similar distractor memory task (SMT). During the target phase, stimuli included either a target (identical to the cue) or a catch stimulus (similar to the cue, not requiring a response). **(Bottom)** Target task-related neural activity (green) was observed in the dorsal anterior cingulate cortex (dACC) and insula (brown). Functional Connectivity: Functional connectivity analysis revealed correlations between the salience network (e.g., dACC and insula; blue) and the noradrenergic locus coeruleus (LC; dark green). Strength of functional connectivity in both dACC-LC and insula-LC was positively associated with individual impulsivity scores.

for the task condition and 200 scans during the resting state. Additionally, we obtained a high-resolution T1-weighted anatomical image using a 3D gradient echo sequence (TR = 2300 ms; TE = 2.52 ms; 1 mm slice thickness, no gap; in-plane resolution of 1 × 1 mm^2; FOV = 256 × 256 x 176 mm^3).

We performed image preprocessing using Statistical Parametric Mapping (SPM12; https://www.fil.ion.ucl.ac.uk/spm/software/spm12/) to address slice-time correction, motion correction, and correction for magnetic field inhomogeneities. Coregistration processes aligned the functional fMRI data to both the whole-brain EPI and the high-resolution anatomical images. The images were subsequently standardized to Montreal Neurological Institute (MNI) space and spatially smoothed using a Gaussian kernel with a full width at half maximum (FWHM) of 6 mm.

Statistics and reproducibility for behavioral data

The behavioral data were analyzed according to the task type (IMT, DMT, and SMT) and stimulus type (target and catch). Task performance, which was measured by accuracy and reaction time, was analyzed using linear mixed-effects models (LMMs) implemented with the "lme4" package in R[40]. These models included task, stimulus, and their interaction as fixed effects, while age and sex were included as covariates. To account for within-subject correlations, random intercepts were specified for individual participants. Statistical significance of fixed effects was assessed using Type III F-tests with Satterthwaite degrees-of-freedom approximation. When significant effects were found, pairwise comparisons based on estimated marginal means were used to test for condition-level differences by task and stimulus. Furthermore, to integrate the reaction time and accuracy into a single dependent variable, we used the rate correct score (RCS), which was calculated as the ratio of the proportion of correctness to the reaction time of clicks at target onset[41], where i refers to the task type and j refers to the participant.

$$RCS_{ij} = \frac{Proportionofcorrectness_{ij}}{Responsetime_{ij}} \quad (1)$$

Additionally, we investigated the correlation between behavioral response and the BIS11 score as well as neural activity and connectivity for each condition. To examine these associations more precisely, partial correlation analyses were conducted for each behavioral measure (error rate, RT, and RCS) statistically controlling for age and sex.

Statistics and reproducibility for neuroimaging data

Task-based fMRI participant-level analysis (1st level)

To detect neural activity related to the interaction effects of the response (i.e., target and catch) and task (i.e., IMT, DMT, and SMT), we estimated a general linear model (GLM) in SPM12 at the participant (first) level and subsequently analyzed contrast images at the group (second) level.

For each participant and trial block, we modeled eight primary events: 1) cue screen onset; 2) target onset (IMT); 3) target onset (DMT); 4) target onset (SMT); 5) catch onset (IMT); 6) catch onset (DMT); 7) catch onset (SMT); and 8) information screen onset. Each event, except the information screen (18 s), was modeled as having a duration of 0.5 s and convolved with canonical basis functions. Additionally, we included six unconvolved motion parameters and a regressor for each block to account for potential confounding factors. Contrasts on the target and catch events for each task type (IMT, DMT, SMT) were used to generate individual contrast images.

Task-based fMRI group-level analysis (2nd level)

To identify the brain regions involved in processing the interaction effects of the response and task, we employed flexible factorial designs with contrast images derived from individual GLM analyses. Whole-brain results are reported at $p < 0.05$, voxel-level FWE-corrected. Regions of interest (ROIs) were specified using the Automated Anatomical Labeling atlas version 3 (AAL3)[42], which focuses on the bilateral insula and dACC. An inclusive mask was applied to the bilateral insula, and an exclusive mask was used for the supplementary motor area (SMA) to minimize motor-related activity interference. This exclusive mask for the SMA was implemented as a methodological control to enhance the specificity of our findings related to cognitive processes rather than motor execution.

Table 1 | Behavioral results ($n = 90$)

	IMT			DMT			SMT			f score	p value
	mean	SE	95% CI	mean	SE	95% CI	mean	SE	95% CI		
Error rate											
Target(Miss)	0.06	0.02	[0.03, 0.10]	0.11	0.02	[0.75, 0.10]	0.13	0.02	[0.10, 0.17]	14.59**	1.4×10^{-6}
Catch(FA)	0.21	0.02	[0.18, 0.25]	0.22	0.02	[0.18, 0.25]	0.18	0.02	[0.15, 0.21]	1.29	0.278
Reaction time (ms)											
Target(Hit)	605.44	16.66	[572.60, 638.28]	632.29	16.66	[599.44, 665.13]	621.96	16.66	[589.12, 654.80]	3.56*	0.030
Catch(FA)	576.22	19.57	[537.73, 614.72]	606.55	18.56	[570.02, 643.09]	632.06	18.68	[595.29, 668.83]	2.07	0.131
Rate Correct Score (RCS)											
Target	0.16	0.003	[0.15, 0.17]	0.15	0.003	[0.14, 0.16]	0.14	0.003	[0.14, 0.15]	15.45**	6.5×10^{-7}

*$p < 0.05$, **$p < 0.001$.

All statistical comparisons were conducted as two-sided post-hoc pairwise t-tests based on the linear mixed-effects model. Sample size: $n = 90$. Statistical significance was defined as $p < 0.05$. *IMT* Immediate-Memory Tasks, *DMT* Delayed-Memory Tasks, *SMT* Similar distractor Memory task, *FA* False Alarm.

Task-modulated functional connectivity between salience network and LC

We assessed task- and stimulus-dependent functional connectivity between the insula and dACC during stimulus trials (target or catch) via generalized psychophysiological interaction (PPI) analysis[43,44]. For each participant, eigenvariate time series were extracted from the bilateral insula and dACC (from group-level analysis), which served as seed regions. These signals were deconvolved to reconstruct a neural activity time series in the seed regions, which functioned as the physiological regressor for the PPI analyses. Psychological regressors included the catch and target conditions for each task (IMT, DMT, SMT), and interaction regressors were created by multiplying the physiological and psychological regressors. Moreover, six motion regressors and block-of-no-interest regressors were included.

Subsequently, we investigated the correlation between catch- or target-related interaction contrast images and individual impulsivity measures (K-BIS-11-R; from section Psychological measurements). For this analysis, we focused on the connectivity between the bilateral insula and dACC given its significance in the salience network[45] to the noradrenergic locus coeruleus (LC). Age and sex were included as covariates to account for their potential influence on connectivity patterns.

Resting-state functional connectivity between salience network and LC

To explore the general relationship between impulsivity and the salience network (e.g., insula and dACC)-LC connectivity, we examined task-independent (i.e., intrinsic) neural activity in the resting-state fMRI session. After standard preprocessing (as described in section Neuroimaging acquisition and preprocessing), the time series were further processed to remove artifact effects. This involved eliminating linear components that corresponded to the six rigid-body motion parameters, as well as the mean time series from white matter, cerebrospinal fluid, and the global brain signal to remove widespread physiological artefacts[46,47]. A bandpass filter (0.009–0.08 Hz) was then applied. We then extracted regional time series data of the preprocessed BOLD signal from both regions. We used an anatomical mask (including bilateral insula—even encompassing the posterior portion—and the dACC) as seeds in our resting-state fMRI seed-based connectivity analyses with the noradrenergic LC and extracted parameter estimates from the entire anatomical regions.

In the individual-level analysis, the functional connectivity strengths between the ROIs and the entire brain were calculated using Pearson's correlation coefficients and converted to z scores via Fisher's r-to-z transformation. Group-level analysis was conducted using one-way t tests on individual Barratt impulsivity scores with a focus on insula–LC and dACC–LC connectivity, which is crucial for salience processing[27–30]. The bilateral insula (Insula_L and Insula_R) and dACC (ACC_Sup_L and ACC_Sup_R) were defined with the AAL3 atlas[42] and the LC ROI was defined with the Keren's standard 2 SD LC mask[48].

As in the task-based connectivity analysis, age and sex were included as covariates to control for potential confound influences on resting-state connectivity.

Results

Behavioral response

For the error rate, there was a main effect of the stimulus type, $F(1445) = 68.59$, $p < 0.001$, $\eta_p^2 = 0.134$ as shown in Table 1 and Fig. 2. Participants showed significantly higher error rates in catch trials than those in target trials ($p < 0.001$). There was a significant interaction effect on the error rate between the task type and the stimulus type, $F(2, 445) = 5.84$, $p < 0.05$, $\eta_p^2 = 0.026$. In target trials, the error rates for DMT and SMT were higher than those for IMT ($t(445) = 2.19$, $p < 0.05$; $t(445) = 3.32$, $p < 0.05$, respectively). However, there were no significant differences between the task types in the catch trials, as shown in Fig. 2A.

With regard to the reaction times, the linear mixed-effects model revealed a main effect of task type, $F(2, 358) = 3.89$, $p < 0.05$, $\eta_p^2 = 0.021$. The reaction times for the DMT and SMT were significantly slower than those for the IMT ($p < 0.05$ for both). The reaction times for false alarms in the SMT were significantly slower than those for the IMT ($t(363) = 2.61$, $p < 0.05$) as shown in Fig. 2B.

Additionally, there was a main effect of task type, $F(2, 178) = 15.45$, $p < 0.001$, $\eta_p^2 = 0.148$, on the RCS of the target stimuli. The RCS for the IMT was greater than that for the DMT and SMT ($t(178) = 4.43$, $p < 0.001$; $t(178) = 5.12$, $p < 0.001$, respectively) as shown in Fig. 2C.

In a partial correlation analysis controlling for age and sex, the K-BIS11-R score revealed significant positive correlations with the error rate in the target stimuli for both the IMT and DMT ($r = 0.30$, $p < 0.05$; $r = 0.22$, $p < 0.05$, respectively) and showed significant positive correlations with false alarms in the catch stimuli for the IMT ($r = 0.22$, $p < 0.05$).

In a subsequent analysis of age effects on behavioral responses, we observed a significant main effect of age, $F(1, 87) = 4.16$, $p < 0.05$. Age was negatively correlated with error rates in the DMT catch trials (see Table S1 in the Supplementary Material for details). However, no significant age effects were observed for reaction times or RCS.

Interaction effects between task and stimulus types on the salience network

We compared contrasts between the stimulus types (e.g., catch or target) across different task categories (e.g., IMT, DMT, or SMT). The analysis revealed significant interaction effects in the salience network, particularly in the bilateral

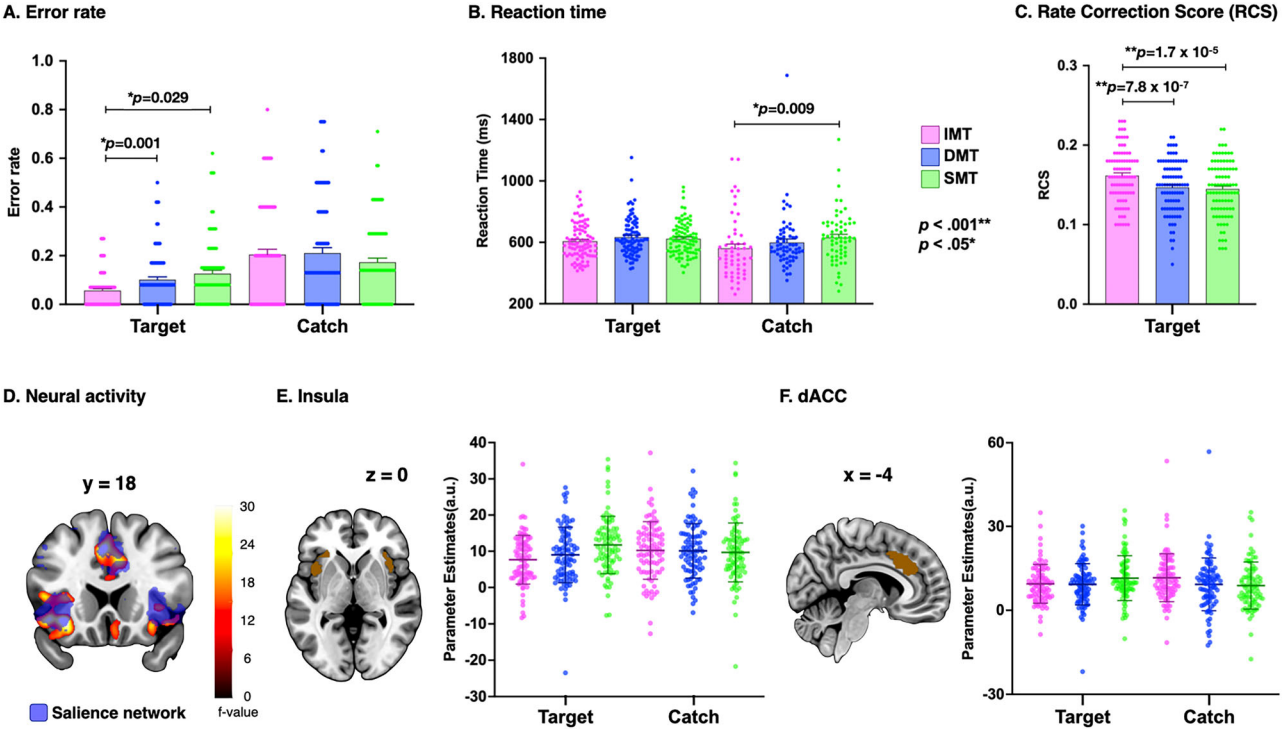

Fig. 2 | Behavioral and neural results of the task. Behavioral results across conditions ($n = 90$). Statistical significance was defined as $p < 0.05$. In the behavioral results, all statistical comparisons were conducted as two-sided post-hoc pairwise t-tests based on the linear mixed-effects model, and error bars represent the standard error of the mean (SEM). **A** The error rate was calculated as the ratio of the number of error trials to the total number of trials. In target trials, the error rates for DMT and SMT were higher than those for IMT ($p = 0.001$, $p = 0.029$, respectively). **B** Response time (in milliseconds) was shown for correct responses during target trials and for error responses during catch trials. The reaction times for false alarms in the SMT were significantly slower than those for the IMT ($p = 0.009$). **C** The rate correct score (RCS) is defined as the ratio of the proportion of correct responses to the average response times for each condition. The RCS for the IMT was greater than that for the DMT and SMT ($p = 7.8 \times 10^{-7}$, $p = 1.7 \times 10^{-5}$, respectively). **D** Neural interaction effects observed within the salience network, particularly in the bilateral anterior insula and dorsal anterior cingulate cortex (dACC), as identified using the Neurosynth keyword "salience network" (blue). **E** Neural responses to the target and catch phase in the bilateral insula. and (**F**) in the dACC (brown), All interaction effects in (**D**) were whole-brain FWE cluster-corrected ($p < 0.05$, cluster-forming threshold: $p < 0.001$). Coordinates for data extraction were determined using group-level results from (**D**), with an inclusive mask of the insular cortex for (**E**) and an exclusive mask of the supplementary motor area (SMA) to minimize motor-related activity for (**F**). Both masks were defined with the Automated Anatomic Labeling at the atlas. Parameter estimates in panels (**E**, **F**) are derived from the significant interaction effects, ensuring that all reported differences are based on independent, whole-brain corrected analyses performed in SPM. Error bars represent the mean and standard deviation (SD), and the color bar represents f-values for the interaction effect.

anterior insula (f = 39.90 for the left; f = 24.19 for the right; whole-brain FWE cluster-level corrected, $p < 0.05$, cluster-forming threshold: $p < 0.001$; Fig. 2D, E; Table 2) and the dorsal anterior cingulate cortex (dACC; f = 27.42; Fig. 2D, F; Table 2). Additional regions that showed interaction effects included the thalamus (f = 32.66 for the left; f = 21.69 for the right), primary motor cortex (precentral gyrus; f = 35.54 for the left; f = 23.32 for the right), supplementary motor area (SMA; f = 38.63), and occipital area (lingual gyrus; f = 29.98), some of which are components of the broader salience network.

We subsequently focused on examining the activity in the bilateral insula and dACC, which are key components of the salience network[45], across different task conditions. In the IMT trials, we observed stronger no-response catch trial signals compared to target response trial signals in the bilateral anterior insula (x = 32, y = 18, z = −12, t = 6.16 for right; x = −30, y = 22, z = −10, t = 5.80 for left) and dACC (x = 10, y = 30, z = 30, t = 5.41) with whole-brain FWE cluster correction. Conversely, in the SMT trials, target response trials induced a stronger response in the bilateral anterior insula (x = −32, y = 18, z = 8, t = 4.88 for left; x = 40, y = 8, z = −2, t = 4.11 for right) and dACC (x = 2, y = 14, z = 38, t = 6.92) than the no-response catch trials. No significant differences were detected in the DMT trials when the catch and target trials were compared in both the anterior insula and dACC regions.

Task-modulated functional connectivity between the insula and dACC

A psychophysiological interaction (PPI) analysis was conducted to explore the task-based functional connectivity between the insula and dACC across different stimulus conditions. The analysis demonstrated significant connectivity between the bilateral insula and dACC during the target phase (t = 7.42; $p < 0.05$, whole-brain FWE cluster-corrected, cluster-forming threshold: $p < 0.001$; Fig. 3A). Notably, stronger connectivity with the dACC was observed across all tasks during the target phase (IMT: t = 4.84; DMT: t = 6.34; SMT: t = 5.97; $p < 0.05$, whole-brain FWE cluster-corrected, cluster-forming threshold: $p < 0.001$). This connectivity was not observed in the catch phase (thresholded at $p < 0.001$). Regarding behavioral performance, the higher the number of false alarms in the SMT catch trials was associated with lower functional connectivity between the insula and the dACC (r = −0.23, $p < 0.05$). After controlling for sex and age, this relationship was maintained as a trending correlation (r = −0.20, $p = 0.06$; Fig. 3B). However, no significant correlation was observed between functional connectivity and the error rate in the target trials of the SMT (r = 0.11, $p = 0.30$).

A parallel PPI analysis using dACC activity as the physiological regressor with the same psychological regressor as above revealed significant connectivity with the bilateral insula during the target phase (t = 7.06 for left; t = 6.68 for right; $p < 0.05$, whole-brain FWE cluster-corrected, cluster-forming threshold: $p < 0.001$; Fig. 3C). During the catch phase, this connectivity was observed only in the left insula (t = 4.06; small-volume FWE peak-corrected, p < 0.05; x = −36, y = 22, z = −2). Additionally, the higher the impulsivity score was associated with the lower the functional connectivity between the dACC and the insula in the catch trial of the DMT (r = −0.26, $p < 0.05$; Fig. 3D). A subsequent analysis of age effects on this

Table 2 | Brain regions interaction effects of response and task ($n = 90$)

Region	Cluster size (# voxels)	Cluster-levelp (FWE)	Mean f statistic	Peak MNI coordinates		
				x	y	z
L. Insula	1183	<0.001	39.90	−32	20	−10
L. IFG triangular part			23.35	−44	18	8
L. SFG medial extending into SMA	1875	<0.001	38.63	−4	16	42
B. ACC supracallosal extending into dorsal ACC			27.42	12	28	24
			18.85	−10	36	16
L. Precentral gyrus	353	<0.001	35.54	−18	−24	56
L. Thalamus MDm	542	<0.001	32.66	−8	−20	8
R. Thalamus Pul			21.69	20	−24	10
L. Hippocampus			15.47	−20	−26	−10
L. Lingual gyrus	2307	<0.001	29.98	−2	−74	0
R. Inferior temporal gyrus			28.65	46	−66	−10
R. Lingual gyrus			25.00	14	−60	4
R. Superior occipital gyrus	1331	<0.001	28.88	22	−82	26
R. Superior parietal gyrus			24.79	26	−56	60
L. Angular gyrus	234	0.003	25.51	−54	−52	34
R. Gyrus rectus	367	<0.001	25.21	6	24	−20
L. Medial orbital gyrus			13.90	−14	28	−18
R. Insula	148	0.028	24.19	32	20	−12
L. Precentral	454	<0.001	23.96	−46	−4	44
L. Middle frontal gyrus			22.01	−28	0	56
R. Precentral gyrus	171	0.014	23.32	22	−24	60
L. Superior parietal gyrus	361	<0.001	22.02	−20	−58	50
L. Inferior parietal gyrus			12.37	−38	−46	52
L. Precuneus			12.09	−6	−44	62
L. Superior occipital gyrus	188	0.009	20.92	−16	−84	26
R. Insula	137	0.038	20.80	32	26	2
R. Parahippocampal gyrus	171	0.014	18.83	30	2	−36

The *p*-values were derived using two-sided ANOVA with post-hoc t-tests. Anatomical labels are based on AAL3. Sample size: $n = 90$. Statistical significance was defined as whole-brain family-wise error rate (FWE) corrected at the cluster-level, $p < 0.05$; cluster-inducing voxel threshold $p < 0.001$. *MNI* Montreal Neurological Institute; *L.* Left, *R.* Right, *B.* Bilateral, *IFG* Inferior frontal gyrus, *SFG* Superior frontal gyrus, *SMA* supplementary motor area, *ACC* Anterior cingulate cortex, *MDm* Mediodorsal medial magnocellular, *Pul* Pulvinar inferior. Gray matter labels are from the AAL3 atlas.

connectivity yielded no significant results for either the insula or dACC seeds.

Functional coupling between the salience network-LC and impulsivity

Our neural findings underscore the crucial role of the salience network, specifically the bilateral insula and dACC, in mediating task-related responses. This analysis revealed that greater impulsivity, as reflected by responses during the target phase across all task categories, was correlated with stronger connectivity to the LC (peak-level FWE small volume corrected within the Keren's 2 SD LC mask[48], threshold and a cluster-forming threshold of $p < 0.005$). The tendency of positive correlation between functional connectivity and impulsivity persisted after controlling for sex and age (bilateral insula-LC: $p = 0.060$; dACC-LC: $p = 0.059$; Fig. 4A, C, green). For the catch phase, the correlations between both the insula-LC and the dACC-LC and impulsivity were not significant.

To further investigate the potential of these couplings as neural biomarkers of impulsivity, we analyzed the correlation between impulsivity and resting-state connectivity (insula-LC and dACC-LC; insula mask from Insula_L Insula_R and dACC mask from ACC_Sup_L ACC_Sup_R in AAL3[24]). In line with our task-induced findings, we observed a positive correlation between impulsivity and resting-state connectivity in these regions (peak-level FWE small-volume corrected within the standard LC mask; Fig. 4B, D). These correlations remained significant after controlling for sex and age (Insula-LC: $p < 0.05$; ACC_Sup-LC: $p = 0.060$; Fig. 4B, D).

With respect to the correlation between behavioral responses and the functional connectivity associated with impulsivity, the stronger the functional connectivity between the dACC and LC was, the higher the error rates in the IMT and DMT of the target trials ($r = 0.22$, $p < 0.05$; $r = 0.28$, $p < 0.05$, respectively) and the greater the number of false alarms in the SMT of the catch trials ($r = 0.25$, $p < 0.05$). The results persisted despite adjustments for age and gender. In additional age-related analysis, we found regions that revealed an inverse correlation between age and functional connectivity in the ACC and insula (see Tables S2 and S3 in Supplementary Material for details).

Discussion

This study employed IMT, DMT, and SMT tasks to investigate adolescent impulsivity and its relationship with neural cognitive control strategies. Neuroimaging data showed that the insula and dACC encode the interaction between response types (target vs. catch) and task conditions (IMT, DMT, and SMT), displaying significant activation and functional connectivity. Additionally, insula-LC and dACC-LC coupling was positively correlated with individual impulsivity scores, suggesting these neural connections as consistent markers of impulsivity. These findings highlight crucial neural mechanisms underlying adolescent impulsivity and offer insights for interventions to reduce risky behaviors.

In this study, we developed and implemented a unique experimental design that extends the previous IMT and DMT paradigms by incorporating an additional SMT condition. By introducing the SMT, which adds visual distractors that closely mimic the target, we aimed to increase cognitive demands and examine the response of the salience network with varying task complexity. This design not only captures impulsivity-related attentional processes, as addressed by the classical IMT and DMT tasks, but also facilitates a detailed analysis of inhibitory control. Specifically, by including catch trials in which participants must withhold responses despite cue-like prompts, we can compare neural activation between successful and failed catch trials, thereby isolating the response inhibition component from the broader attentional processes.

The adolescent participants exhibited higher error rates for the target stimulus in both the DMT and SMT conditions compared to the IMT condition. However, there was no significant difference in performance for the catch stimulus across the tasks. The observed behavioral outcomes indicate that distinct cognitive processes are used for different memory tasks. Moreover, highly impulsive adolescents made more errors in the IMT and DMT. However, no significant relationship was detected between impulsivity and performance in the SMT. These findings suggest that the impact of impulsivity on behavioral performance can differ depending on the specific distractor. In the correlation results between impulsivity and behavioral responses, higher impulsivity was associated with lower rates of correct responses in the target trials of the IMT and DMT. Higher impulsivity among adolescents was also associated with higher false alarms in the catch trials of the IMT. The more banal and monotonous the distracting stimuli are (e.g., 12345), the more difficult it is to maintain attention, which leads to a higher incidence of response errors. The negative correlations between impulsivity and response consistency highlight the struggles faced by adolescents in tasks that demand

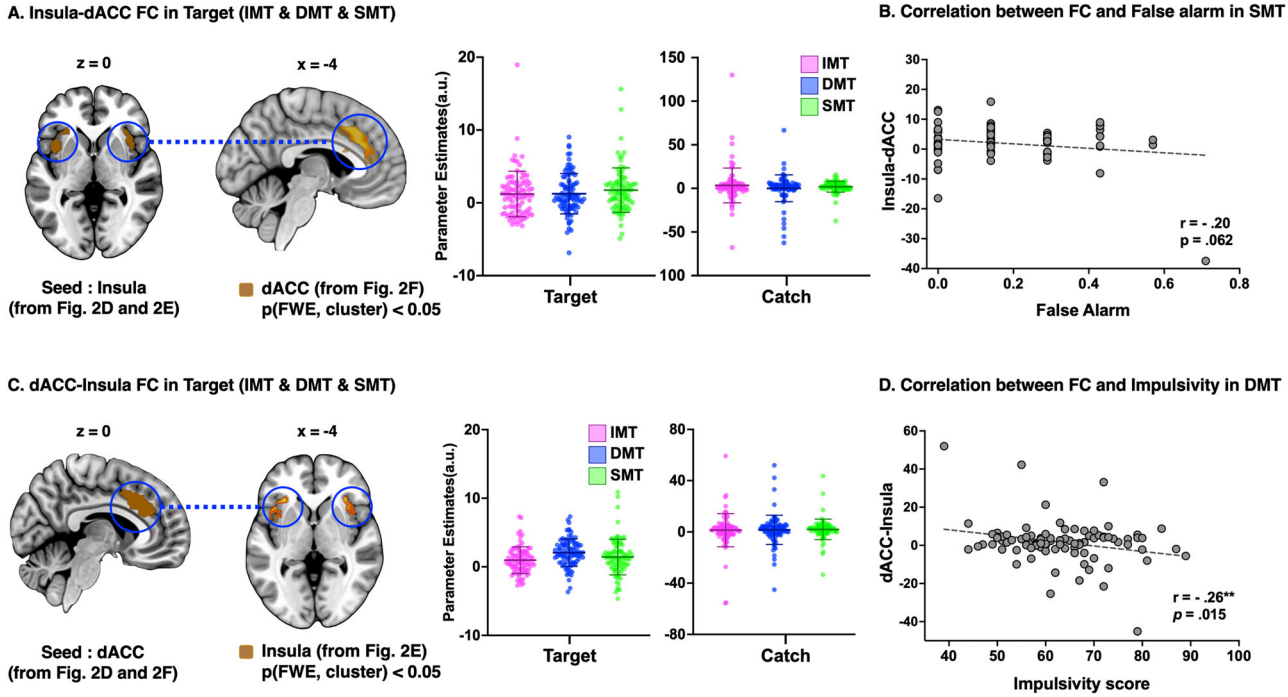

Fig. 3 | Functional coupling between the insula and dACC during the task. Neural correlations were whole-brain voxel-level family wise error (FEW) corrected $p < 0.05$ for (**A**, **C**) (bilateral insula mask from Fig. 2E; dACC mask from Fig. 2F). Error bars represent the mean and standard deviation (SD) ($n = 90$). **A** Psychophysiological interaction (PPI) analysis using the bilateral insula (from Fig. 2E; brown) as the seed region revealed significant connectivity (family wise error (FWE) cluster-level corrected $p < 0.001$) with the dorsal anterior cingulate cortex (dACC; from Fig. 2F; brown) during all target phases (i.e., IMT, DMT, and SMT) as well as during each individual task. Estimated PPI betas in dACC were derived from each individual phase ($n = 90$). **B** The negative correlation tendency between functional connectivity and the number of false alarms in the SMT catch trials persisted after adjusting for sex and age, as confirmed by two-tailed Pearson correlation analyses (r = −0.20, $p = 0.062$; $n = 90$; **B**). **C** Similarly, when the dACC was used as the seed region, significant connectivity (FWE cluster-level corrected $p < 0.001$) with the bilateral insula was observed during all target phases as well as during each individual task. Estimated PPI betas in bilateral insula were derived from all target phases each individual phase ($n = 90$). **D** Two-tailed Pearson correlation analyses showed that the impulsivity score was associated with the lower functional connectivity between the dACC and the insula in the catch trial of the DMT (r = −0.26, $p = 0.015$; $n = 90$). All reported effects are based on independent, corrected analyses.

quick decision-making and response inhibition. Individuals with ADHD generally display a greater incidence of mistakes in simpler activities while showcasing enhanced performance in more complicated tasks[49]. Thus, the level of motivation and concentration in relation to the complexity of a task affects performance in activities linked to impulsivity.

Our results demonstrate that this expanded task design effectively modulates activity within key regions of the salience network, particularly the insula and dACC. At the time of the target phase, the functional coupling between the anterior insula and dACC was significant in all task categories, whereas at the time of the catch phase, it was weakly or preferentially coupled in the more cognitively demanding SMT task. Previous research has established both anatomical[50–54] and functional[23–25,55] connections between the insula and the dACC and has highlighted their importance in integrating internal and external stimuli to influence behavior. This finding contributes to a deeper understanding of the communication between these regions, particularly in the context of response inhibition and task complexity. The robust dACC-insula connectivity during response trials suggests that these regions coordinate closely when a response is required, while the diminished connectivity during response inhibition phases indicates a preferential increase in cognitive demands when withholding responses in these scenarios. These findings extend our understanding of the functional dynamics between the dACC and insula and emphasize their critical role in tasks that require high levels of cognitive control.

The significant engagement of the salience network across the IMT, DMT, and SMT conditions suggests that this experimental approach is robust for studying the neural correlates of impulsivity, especially in adolescent populations for whom self-regulation and risk-taking behaviors are of particular concern.

In the SMT, with distractor stimuli modulated to resemble the target and catch stimuli, adolescents who made more false alarms in the catch phase exhibited reduced functional connectivity between the insula and dACC and between the insula and LC. In contrast, there was no correlation between errors in the target stimulus and functional connectivity. These findings indicate that adolescents engage different types of functional connectivity depending on their task performance strategy and that these cognitive strategies have an impact on behavioral results. The observed modulation is consistent with prior studies that highlight the involvement of these regions in tasks that require heightened cognitive control and decision-making under uncertainty[56,57].

The integration of the SMT into the traditional IMT/DMT framework represents a meaningful advance in experimental design. It provides a more nuanced understanding of how the brain processes different levels of cognitive demand and task difficulty, particularly in relation to impulsivity. Moreover, the ability of the SMT to consistently engage the salience network supports its utility in future research that aims to develop neural biomarkers for impulsivity and related behaviors.

In this study, we explored potential behavioral and neural biomarkers of adolescent impulsivity using an experimental task design as well as task-independent (i.e., resting-state fMRI) neural coupling. Previous research that has leveraged advanced neuroimaging techniques has begun to elucidate the neural underpinnings of these phenomena. For example, Van Den Bos and colleagues demonstrated that enhanced connectivity within the frontostriatal circuits is inversely related to impulsive decision-making[58]. These results underscore the necessity of integrating the neurodevelopmental and socioemotional dimensions to fully understand behavioral manifestations during adolescence[3,59]. Analyzing these interactions provides

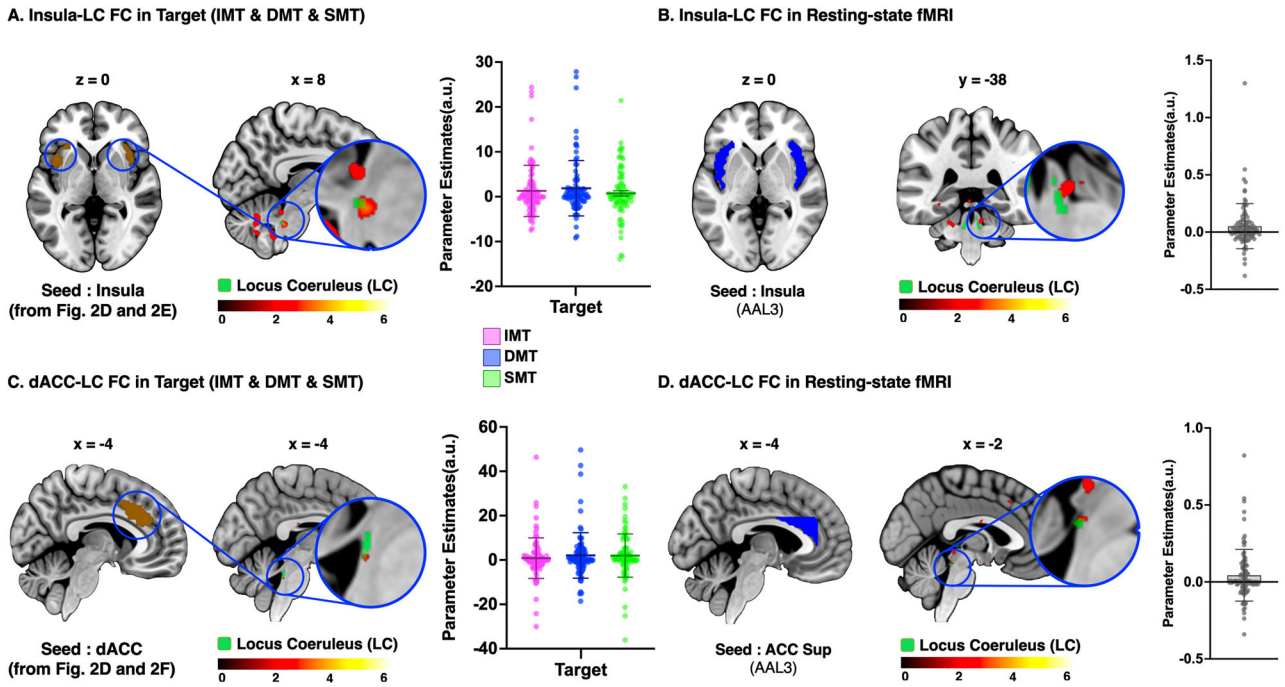

Fig. 4 | Positive correlation of insula-LC and dACC-LC coupling with impulsivity in target task-induced and task-independent conditions. Positive correlation of functional connectivity with impulsivity ($n = 90$). Statistical significance was assessed using a one-sided t-contrast (activation > 0) at a cluster-forming threshold of $p < 0.005$, FWE small-volume-corrected at the peak level. **A** PPI analysis using the bilateral insula as the seed region revealed a positive correlation between impulsivity, as measured by the Barratt Impulsiveness Scale (BIS-11), and insula-locus coeruleus (LC) connectivity during all target phases (peak-level FWE small-volume corrected within the LC, with a cluster-forming threshold of $p < 0.005$; $n = 90$). Estimated interaction betas of PPI and individual impulsivity in LC for each individual target phase. **B** In the resting-state condition, a positive correlation was also observed between impulsivity and insula-LC connectivity (peak-level FWE small-volume corrected within the LC). **C** A positive correlation was noted between impulsivity and dACC-LC connectivity during target response trials (peak-level FWE small-volume corrected within the LC). The graph shows the estimated PPI interaction betas for LC connectivity and individual impulsivity scores during these trials. **D** A weak positive correlation between impulsivity and dACC-LC connectivity was identified in the resting-state condition (peak-level FWE small-volume corrected within the LC). The insula and dACC ROIs from Fig. 2D, E for (**A**, **C**) were defined with the Automated Anatomic Labeling Atlas (blue) for (**B**, **D**). We defined the LC ROI using the standard LC mask, Keren's 2 SD LC (green). Error bars represent the mean and standard deviation (SD). The color bar represents t-values for the correlation between connectivity and impulsivity.

essential insights into the complexities of adolescent impulsivity and its implications for developmental trajectories.

Notably, given the critical role of the salience network and the LC in salience processing[27–30], we focused on examining the coupling between these regions and their relationships with impulsivity, as measured by the BIS-11[33] during the target and catch phases. We observed that this coupling varies with the level of impulsivity. The excessive functional connectivity between the dACC and LC, which is related to impulsivity, was associated with lower correct answer rates in the IMT and DMT of the target trials and higher false alarms in the SMT of the catch trials. This finding is consistent with the finding that greater impulsivity is associated with lower behavioral performance in the IMT and DMT of target trials and in the SMT of catch trials.

We observed that connectivity between the insula and LC, as well as between the dACC and LC, was correlated with impulsivity in both the target phase and the resting state. This consistency across both rest and task is important for our findings. The brain's baseline connectivity is thought to provide a "blueprint" for its function during active tasks[60]. Finding the same brain-behavior relationship in both conditions makes our conclusions more robust, suggesting this link is a stable biological trait rather than a temporary reaction to the task[61]. Therefore, the coupling between the salience network[18] and the noradrenergic LC may serve as a reliable neural marker for impulsivity. Given the known relationship of the LC with pupil dilation[62,63], future studies could explore the use of pupilometry as a noninvasive biomarker for assessing impulsivity. Such an approach could offer a portable and practical tool for both research and clinical applications.

Overall, our findings demonstrate that our task design, combined with both task-specific and general connectivity measures, provides a promising framework for identifying adolescent impulsivity through behavioral and neural markers. This approach can contribute to the development of effective strategies for assessing and managing impulsivity-related behaviors in adolescents. Our study's cross-sectional design limits our ability to infer developmental changes over time. Although our sample of 90 adolescents is robust for task-based fMRI, the gender distribution is imbalanced, with only 24 female participants, which may affect the generalizability of our findings. Notably, our resting-state connectivity analyses revealed a significant association between bilateral insula–LC connectivity and impulsivity, whereas the task-modulated connectivity between these regions was only marginally significant. Future research employing longitudinal designs, larger and more balanced samples, and various personalized data will be crucial to further validate and extend these findings. Despite these limitations, our research offers useful perspectives on the neural mechanisms underlying impulsivity, contributing to the development of effective strategies for assessing and managing impulsivity-related behaviors in adolescents.

Data availability

The numerical source data underlying the graphs and statistical analyses presented in the main figures are provided as Supplementary Data in Excel format. The Excel file contains separate sheets for each figure (Figs. 2–4), and the mean and SEM values are available in Supplementary Tables 4–6. The data that support the findings of this study are available on reasonable request from the corresponding author, J-W.C. The raw datasets are not publicly available, as they contain information that could compromise research participant privacy and consent. All data are securely stored on encrypted institutional servers at the Catholic University of Korea College of Medicine. Data requests should be directed to the corresponding author (email: jwchun@catholic.ac.kr), who will respond within four weeks. Access

will be granted for academic purposes only, in accordance with institutional and ethical regulations.

Received: 25 January 2025; Accepted: 21 October 2025;
Published online: 27 November 2025

References

1. Butler, G. K. L. & Montgomery, A. M. J. Impulsivity, risk taking and recreational 'ecstasy' (MDMA) use. *Drug Alcohol Depend.* **76**, 55–62 (2004).
2. Slutske, W. S., Caspi, A., Moffitt, T. E. & Poulton, R. Personality and Problem Gambling. *Arch. Gen. Psychiatry* **62**, 769–769 (2005).
3. Smith, A. R., Chein, J. & Steinberg, L. Impact of socio-emotional context, brain development, and pubertal maturation on adolescent risk-taking. *Hormones Behav.* **64**, 323–332 (2013).
4. Twisk, D. A. M. & Stacey, C. Trends in young driver risk and countermeasures in European countries. *J. Saf. Res.* **38**, 245–257 (2007).
5. Steinberg, L. A social neuroscience perspective on adolescent risk-taking. *Developmental Rev.* **28**, 78–106 (2008).
6. Casey, B. J. et al. Behavioral and neural correlates of delay of gratification 40 years later. *Proc. Natl. Acad. Sci. USA* **108**, 14998–15003 (2011).
7. Gökçearslan, Ş, Mumcu, F. K., Haşlaman, T. & Çevik, Y. D. Modelling smartphone addiction: The role of smartphone usage, self-regulation, general self-efficacy and cyberloafing in university students. *Computers Hum. Behav.* **63**, 639–649 (2016).
8. Constantinidis, C. & Luna, B. Neural Substrates of Inhibitory Control Maturation in Adolescence. *Trends Neurosci.* **42**, 604–616 (2019).
9. Vara, A. S., Pang, E. W., Vidal, J., Anagnostou, E. & Taylor, M. J. Neural mechanisms of inhibitory control continue to mature in adolescence. *Developmental Cogn. Neurosci.* **10**, 129–139 (2014).
10. Geier, C. F., Terwilliger, R., Teslovich, T., Velanova, K. & Luna, B. Immaturities in reward processing and its influence on inhibitory control in adolescence. *Cereb. Cortex* **20**, 1613–1629 (2010).
11. Ordaz, S. J., Foran, W., Velanova, K. & Luna, B. Longitudinal growth curves of brain function underlying inhibitory control through adolescence. *J. Neurosci.* **33**, 18109–18124 (2013).
12. Quach, A. et al. Adolescent development of inhibitory control and substance use vulnerability: A longitudinal neuroimaging study. *Developmental Cogn. Neurosci.* **42**, 100771 (2020).
13. Uddin, L. Q., Supekar, K. S., Ryali, S. & Menon, V. Dynamic reconfiguration of structural and functional connectivity across core neurocognitive brain networks with development. *J. Neurosci.* **31**, 18578–18589 (2011).
14. Menon, V. Developmental pathways to functional brain networks: emerging principles. *Trends Cogn. Sci.* **17**, 627–640 (2013).
15. Uddin, L. Q. Salience processing and insular cortical function and dysfunction. *Nat. Rev. Neurosci.* **16**, 55–61 (2015).
16. Heller, A. S. & Casey, B. J. The neurodynamics of emotion: Delineating typical and atypical emotional processes during adolescence. *Developmental Sci.* **19**, 3–18 (2016).
17. Logan, G. D. & Cowan, W. B. On the ability to inhibit thought and action: A theory of an act of control. *Psychol. Rev.* **91**, 295–327 (1984).
18. Menon, V. & Uddin, L. Q. Saliency, switching, attention and control: a network model of insula function. *Brain Struct. Funct.* **214**, 655–667 (2010).
19. Allman, J. M. et al. The von Economo neurons in frontoinsular and anterior cingulate cortex in great apes and humans. *Brain Struct. Funct.* **214**, 495–517 (2010).
20. Aron, A. R., Robbins, T. W. & Poldrack, R. A. Inhibition and the right inferior frontal cortex. *Trends Cogn. Sci.* **8**, 170–177 (2004).
21. Gilzenrat, M. S., Nieuwenhuis, S., Jepma, M. & Cohen, J. D. Pupil diameter tracks changes in control state predicted by the adaptive gain theory of locus coeruleus function. *Cogn., Affect. Behav. Neurosci.* **10**, 252–269 (2010).
22. Murphy, P. R., O'Connell, R. G., O'Sullivan, M., Robertson, I. H. & Balsters, J. H. Pupil diameter covaries with BOLD activity in human locus coeruleus. *Hum. Brain Mapp.* **35**, 4140–4154 (2014).
23. Janes, A. C., Farmer, S., Peechatka, A. L., Frederick, B. D. B. & Lukas, S. E. Insula-dorsal anterior cingulate cortex coupling is associated with enhanced brain reactivity to smoking cues. *Neuropsychopharmacology* **40**, 1561–1568 (2015).
24. Ghahremani, D. G. et al. Functional connectivity of the anterior insula during withdrawal from cigarette smoking. *Neuropsychopharmacology* **46**, 2083–2089 (2021).
25. Cai, W. et al. Causal interactions within a frontal-cingulate-parietal network during cognitive control: convergent evidence from a multisite-multitask investigation. *Cereb. Cortex* **26**, 2140–2153 (2016).
26. Svensson, T. H., Dahlöf, C., Engberg, G. & Hallberg, H. Central pre- and postsynaptic monoamine receptors in antidepressant therapy. *Acta Psychiatr. Scandinavica* **63**, 67–78 (1981).
27. Aston-Jones, G. & Cohen, J. D. An integrative theory of locus coeruleus-norepinephrine function: adaptive gain and optimal performance. *Annu. Rev. Neurosci.* **28**, 403–450 (2005).
28. Neal, J., Song, I., Katz, B. & Lee, T. H. Association of intrinsic functional connectivity between the locus coeruleus and salience network with attentional ability. *J. Cogn. Neurosci.* **35**, 1557–1569 (2023).
29. Navratilova, E. & Porreca, F. Reward and motivation in pain and pain relief. *Nat. Neurosci.* **17**, 1304–1312 (2014).
30. Song, A. H. et al. Pharmacological modulation of noradrenergic arousal circuitry disrupts functional connectivity of the locus ceruleus in humans. *J. Neurosci.* **37**, 6938–6945 (2017).
31. McBurney-Lin, J., Vargova, G., Garad, M., Zagha, E. & Yang, H. The locus coeruleus mediates behavioral flexibility. *Cell Rep.* **41**, 111534 (2022).
32. Dougherty, D. M., Marsh, D. M. & Mathias, C. W. Immediate and delayed memory tasks: A computerized behavioral measure of memory, attention, and impulsivity. *Behav. Res. Methods, Instrum., Computers* **34**, 391–398 (2002).
33. Patton, J. H., Stanford, M. S. & Barratt, E. S. Factor structure of the barratt impulsiveness scale. *J. Clin. Psychol.* **51**, 768–774 (1995).
34. Pechorro, P., Ayala-Nunes, L., Ray, J. V., Nunes, C. & Gonçalves, R. A. The Barratt Impulsiveness Scale-11 Among a School Sample of Portuguese Male and Female Adolescents. *J. Child Fam. Stud.* **25**, 2753–2764 (2016).
35. Martínez-Loredo, V., Fernández-Hermida, J. R., Fernández-Artamendi, S., Carballo, J. L. & García-Rodríguez, O. Spanish adaptation and validation of the Barratt Impulsiveness Scale for early adolescents (BIS-11-A). *Int. J. Clin. Health Psychol.* **15**, 274–282 (2015).
36. Bhat, N. A., Roopesh, B. N., Bhaskarapillai, B. & Benegal, V. Validation of the Barratt Impulsiveness Scale- short form among Indian adolescents. *Asian J. Psychiatry* **37**, 172–177 (2018).
37. Charles, N. E., Floyd, P. N. & Barry, C. T. The Structure, Measurement Invariance, and External Validity of the Barratt Impulsiveness Scale–Brief in a Sample of At-Risk Adolescents. *Assessment* **28**, 116–127 (2021).
38. Lee, S.-R. et al. The Study on Reliability and Validity of Korean Version of the Barratt Impulsiveness Scale-11-Revised in Nonclinical Adult Subjects. *J. Korean Neuropsychiatr. Assoc.* **51**, 378–386 (2012).
39. Stanford, M. S. et al. Fifty years of the Barratt Impulsiveness Scale: An update and review. *Personal. Individ. Differences* **47**, 385–395 (2009).
40. Bates, D., Mächler, M., Bolker, B. M. & Walker, S. C. Fitting linear mixed-effects models using lme4. *J. Stat. Softw.* **67**, 1–48 (2015).
41. Vandierendonck, A. On the utility of integrated speed-accuracy measures when speed-accuracy trade-off is present. *J. Cogn.* **4**, 22 (2020).

42. Rolls, E. T., Huang, C.-C., Lin, C.-P., Feng, J. & Joliot, M. Automated anatomical labelling atlas 3. *NeuroImage* **206**, 116189 (2020).
43. Friston, K. J. et al. Psychophysiological and Modulatory Interactions in Neuroimaging. *NeuroImage* **6**, 218–229 (1997).
44. Gitelman, D. R., Penny, W. D., Ashburner, J. & Friston, K. J. Modeling regional and psychophysiologic interactions in fMRI: the importance of hemodynamic deconvolution. *NeuroImage* **19**, 200–207 (2003).
45. Menon, V. Salience Network. In *Brain Mapping* 597–611 (Elsevier, 2015). https://doi.org/10.1016/B978-0-12-397025-1.00052-X.
46. Murphy, K. & Fox, M. D. Towards a consensus regarding global signal regression for resting state functional connectivity MRI. *NeuroImage* **154**, 169–173 (2017).
47. Liu, T. T., Nalci, A. & Falahpour, M. The global signal in fMRI: Nuisance or Information?. *NeuroImage* **150**, 213–229 (2017).
48. Keren, N. I., Lozar, C. T., Harris, K. C., Morgan, P. S. & Eckert, M. A. In vivo mapping of the human locus coeruleus. *NeuroImage* **47**, 1261–1267 (2009).
49. Boot, N., Nevicka, B. & Baas, M. Creativity in ADHD: Goal-Directed Motivation and Domain Specificity. *J. Atten. Disord.* **24**, 1857–1866 (2020).
50. Showers, M. J. C. & Lauer, E. W. Somatovisceral motor patterns in the insula. *J. Comp. Neurol.* **117**, 107–115 (1961).
51. Wiech, K., Jbabdi, S., Lin, C. S., Andersson, J. & Tracey, I. Differential structural and resting state connectivity between insular subdivisions and other pain-related brain regions. *Pain* **155**, 2047–2055 (2014).
52. Van Den Heuvel, M. P., Mandl, R. C. W., Kahn, R. S. & Hulshoff Pol, H. E. Functionally linked resting-state networks reflect the underlying structural connectivity architecture of the human brain. *Hum. Brain Mapp.* **30**, 3127–3141 (2009).
53. Sotiropoulos, S. N. et al. Advances in diffusion MRI acquisition and processing in the Human Connectome Project. *NeuroImage* **80**, 125–143 (2013).
54. Gogolla, N. The insular cortex. *Curr. Biol.* **27**, R580–R586 (2017).
55. Supekar, K. & Menon, V. Developmental maturation of dynamic causal control signals in higher-order cognition: A neurocognitive network model. *PLoS Comput. Biol.* **8**, 1002374 (2012).
56. Shenhav, A., Botvinick, M. M. & Cohen, J. D. The Expected Value of Control: An Integrative Theory of Anterior Cingulate Cortex Function. *Neuron* **79**, 217–240 (2013).
57. Wu, T. et al. Anterior insular cortex is a bottleneck of cognitive control. *NeuroImage* **195**, 490–504 (2019).
58. Van Den Bos, W., Rodriguez, C. A., Schweitzer, J. B. & McClure, S. M. Adolescent impatience decreases with increased frontostriatal connectivity. *Proc. Natl. Acad. Sci. USA* **112**, E3765–E3774 (2015).
59. Pfeifer, J. H. & Allen, N. B. Arrested development? Reconsidering dual-systems models of brain function in adolescence and disorders. *Trends Cogn. Sci.* **16**, 322–329 (2012).
60. Cole, M. W., Bassett, D. S., Power, J. D., Braver, T. S. & Petersen, S. E. Intrinsic and Task-Evoked Network Architectures of the Human Brain. *Neuron* **83**, 238–251 (2014).
61. Tavor, I. et al. Task-free MRI predicts individual differences in brain activity during task performance. *Science* **352**, 216–220 (2016).
62. Grueschow, M. et al. Real-world stress resilience is associated with the responsivity of the locus coeruleus. *Nat. Commun.* **12**, 2275 (2021).
63. Grueschow, M., Kleim, B. & Ruff, C. C. Functional Coupling of the Locus Coeruleus Is Linked to Successful Cognitive Control. *Brain Sci.* **12**, 305 (2022).

Acknowledgements

This research was supported by the Bio&Medical Technology Development Program of the National Research Foundation (NRF) funded by the Korean government (MSIT) (RS-2023-00223559) and the Basic Medical Science Facilitation Program through the Catholic Medical Center of the Catholic University of Korea funded by the Catholic Education Foundation. Also, J-CK received a Doc.Mobility fellowship (P1ZHP1_184166) from the Swiss National Science Foundation. We thank Sunghyon Kyeong and Suji Chung for helpful discussions.

Author contribution

J-W.C. and D-J.K. contributed to the conception and design of the study. J.K. and J.I.K. contributed to the acquisition of the behavioral and imaging data. J-C.K., J-W.C., and K.S.S. performed the behavioral and imaging data analysis. J-C.K. and J-W.C. wrote the manuscript text and prepared the figures and tables. K.S.S. and M.H. assisted with the interpretation of the data and contributed to the final draft of the manuscript. I.Y.C., T.M.K., and D-J.K. contributed to critically revising the manuscript for important intellectual content. All the authors contributed to the manuscript and approved the final manuscript.

Competing interests

The authors declare no competing interests.

Additional information

Supplementary information The online version contains supplementary material available at https://doi.org/10.1038/s43856-025-01212-y.

Correspondence and requests for materials should be addressed to Ji-Won Chun.

Peer review information *Communications Medicine* thanks Daniel Petrie, Yu Chen, and the other, anonymous, reviewer(s) for their contribution to the peer review of this work.